Wind Energy Systems 2024/25
Individual Coursework

Lingges Shaswat

1. DESIGN A PITCH CONTROL SCHEDULE

1.1 Pitch Control Schedule

To design an effective pitch control schedule, dynamic simulations were conducted using the RNA model in Ashes under uniform flow conditions for the WES 18-MW turbine. The schedule was designed with the operational regions: cut-in, ramp-up, rated and cut-out with wind speeds and pitch angles summarised in Table 1. The cut-in speed of 3.5m/s was selected as it was the minimum wind speed at which electrical power generation initiates from simulation, and a cut-out speed of 25m/s was determined by using similar scaled existing wind turbines and adhering to the IEC Class 1 turbine safety limits [1]. Below the cut-in speed the turbine remains idle where the blades are pitched to 0° and then increased to 3° at the cut-in speed to initiate rotation. It has a linear decrease of pitch angle from 3° to 0°. During the ramp up region, from 9m/s to 12.5m/s, the pitch angle was maintained to be 0° to maximize power coefficient (C_P) and operate at the optimum tip-speed ratio (TSR). Above the rated windspeed, the pitch angle increases to regulate power generated at 18MW to maintain constant torque and RPM. At cut-out, the blades feather to around 90° to prevent overloading the blades to protect the turbine from structural failure and fatigue loads under high wind speeds.

1.1.1 Determining the Cut-in Pitch Angle

To determine the most effective cut-in pitch angle at 3.5m/s, simulations were conducted for a range of pitch angles from 0° to 5° as shown in Figure 1. Most similar sized turbines, shown in Table 2, have a cut-in speed ranged from 3m/s to 4m/s and a cut-out speed of 25m/s as this was taken as an initial value but simulations confirmed it [2].

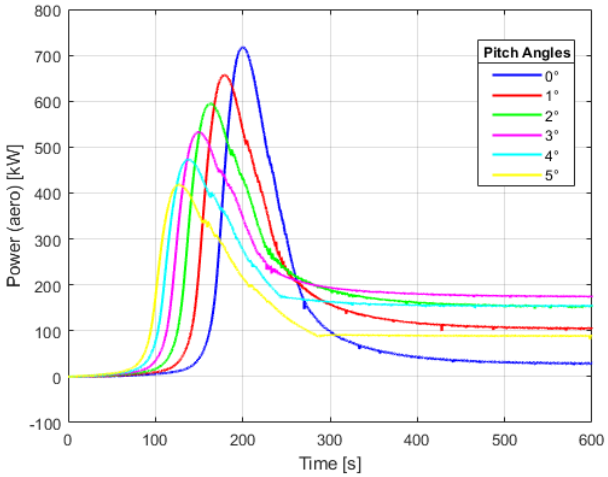

***Figure 1**: Cut-In Pitch Angles at 3.5m/s*

***Table 1**: Pitch Control Schedule*

Wind Speed	Region	Pitch
< 3.5m/s	Idle	0°
3.5 m/s	Cut-In	3°
9.0 m/s	Ramp-Up	0°
12.5 m/s	Rated	0°
25 m/s	Cut-Out	20.64°
> 25m/s	Feather	~90°

At 0° pitch angle the highest peak power was produced, reflecting maximum aerodynamic lift due to optimal blade alignment with the oncoming flow. However, power decayed rapidly indicating insufficient rotational momentum. The higher pitch angles exhibited lower peaks and a shorter startup time than 0° and settle at a steady power output range of 100kW-190kW showing there is some sustained energy capture. These pitch angles were evaluated to balance startup dynamics and steady-state power. The 3° pitch angle emerged as the optimal choice as it achieved a relatively short startup time of 150s, and, critically, the highest steady-state power of approximately 190 kW after 600 seconds. This angle was leveraging sufficient lift while avoiding excessive stalling or drag penalties. The selection of 3° as the cut-in pitch angle

optimizes the turbine's ability to initiate rotation and power generation at the cut-in wind speed of 3.5m/s.

1.1.2 Analysis of Power Curves

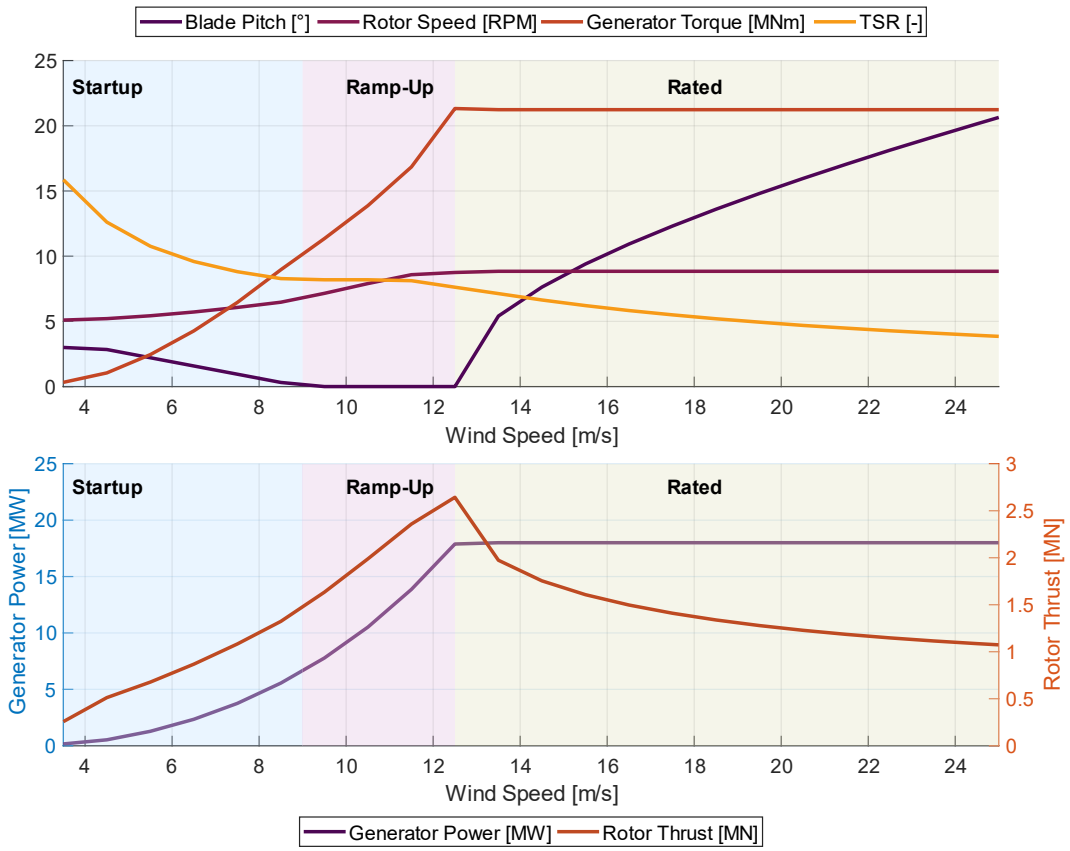

***Figure 2**: Power Curves with (a) Pitch Angle, Rotor Speed, Torque and TSR (b) Power and Thrust with respect to Wind Speed*

The power curves were designed by running manual simulations across a range of windspeeds from 3.5m/s to 25m/s achieving the three shaded regions of cut-in, ramp-up and rated shown in Figure 2. This turbine has a constant pitch angle of 0° in the ramp-up region to maximize C_P of 0.44 and slowly increasing above the rated windspeed to maintain the rated power of 18MW.

1.2.1 Start-Up

Below the cut-in speed, the wind speed is not sufficient to generate any power as there is no torque from the wind to the blades, so the blades remain with a pitch angle of 0°. At the cut-in speed of 3.5m/s the pitch angle starts from 3° and gradually decreases to 0° as windspeed increases to 9m/s. This is to optimize the angle of attack to initiate the rotation as so that the TSR can be reduced and consequently increase C_P to reach a maximum value as soon as possible. The blades generate enough torque to initiate the rotation of the rotor.

1.2.2 Ramp-Up

In this region, the pitch angle stays constant as it needs to maintain the TSR to maximize power generation (C_P), as power generated increases cubically with wind speed ($P \propto u^3$). The 0° pitch maximizes the angle of attack and minimises the drag to fully exploit the aerofoil as higher wind speeds generate higher rotor speeds. The RPM increases linearly towards 8.84 RPM. Due to the increase in wind speed the thrust continues to increase.

1.2.3 Rated

Beyond the rated windspeed of 12.5m/s the objective of the turbine is to generate constant power. This is achieved by maintaining a constant torque of 21MNm and a rotor speed of 8.84 RPM by increasing the pitch angles as windspeed increases shown by $P = Q\omega$. The PID controller was used to control the pitch angles so that the angle of attack of the blade will increase and thus decrease the lift force so that the thrust reduces. When the windspeed exceeds the cut-out speed the turbine will shut down and the blades will pitch to a near 90° angle to feather and to minimise the aerodynamic loads and prevent excessive loading to ensure the structural integrity of the turbine.

1.3 Rotor Diameter Suitability

This rotor diameter of 208m is suited to high wind speed sites because of the cubic dependence of the power output on the wind speed as shown in Equation 1.3. At 12.5m/s the turbine achieves its rated power of 18MW but at lower speeds at 10.5m/s the power output drops to 10.5MW. A larger rotor will capture more wind energy but also needs a sufficient windspeed to generate to the rated power efficiently.

$$P = \frac{1}{2}\rho A v^3 \quad (1.3)$$

At lower wind speed sites, the turbine will struggle to reach the rated power as the cubic relationship is powerful. Thus, the turbine is said to be underutilized and wouldn't reach provide the rated power of 18MW. Moreover, it will also be unable to reach the rated power because of the insufficient aerodynamic force acting on the blades. TSR must be maintained within an optimal range to ensure efficiency but at lower wind speeds the turbine must either require excessive pitch control or spin at a lower RPM to achieve a high TSR. For this rated power of 18 MW, similar turbines are much larger with a rotor diameter of around 260m. This turbine is much smaller compared to it and proving it to be better at capturing energy as it has a higher power density. Power density is how much power a turbine produces over the swept area and is shown in Table 2. This turbine is the most efficient as it produces the most energy with respect to its size. Thus, it is more suited to a higher wind speed area as the bigger swept area of a turbine has the ability to capture more energy at lower wind speeds.

***Table 2**: Comparison with similar rated turbines [3][4][5]*

Model	Rated Power	Rotor Diameter	Swept Area	Power Density
WES 18-MW	18 MW	208 m	33987 m²	0.53 kW/m²
MingYang MySE	16 MW	242 m	45995 m²	0.35 kW/m²
GE Haliade-X	14 MW	220 m	38013 m²	0.37 kW/m²
Siemens Gamesa	14 MW	222 m	38655 m²	0.36 kW/m²

1.3.1 Potential Rotor Design Changes for Lower Wind Speed Sites

To make this turbine more suitable for lower wind speed sites, the rotor diameter could be increased and consequently enlarging the swept area so that it can capture more energy at lower wind speeds. A small increase in rotor diameter will lead to a greater swept area because the turbine intercepts more wind even at lower speeds to generate power. Longer and larger blades create more torque due to the increase in the moment arm. Thus, it is easier for the turbine to rotate at lower wind speeds and will also reduce the cut-in speed. Using longer and slimmer blades to reduce drag at lower wind speeds and consequently increasing the lift to drag ratio for lower windspeeds. Also, the blades mass can be reduced by using carbon fibre instead of fibreglass, so that the turbine can start easier with lower wind speeds. Using carbon fibre composites instead of traditional fiberglass reduces the blade mass despite the increase in length.

1.3.2 Design Implications on the Tower and Foundation

As the swept area increases there is more thrust loading on the tower especially in the ramp-up region. Moreover because of the longer blades it will also create a larger bending moment at the hub which will transfer to the tower. To mitigate this, the tower must be taller and stiffer so stronger materials or thicker steel sections will be required to withstand the increased flapwise loads. The tower has to be taller to increase the tip blade clearance because the blades are longer. Dynamic stability becomes more critical as larger blades create more aerodynamic forces. Increased fatigue loads will also be experienced due to larger and more frequent blade deflections. A larger rotor lowers the natural frequency of the turbine which may align with the wind or wave induced excitation frequencies and this would lead to resonance and structural fatigue. The rotor's increased torque and the taller, heavier tower significantly raise the loading on the foundation. As this is an offshore turbine, larger wave and wind drag forces will affect the structure. As a result, larger and deeper monopiles are required with more seabed penetration to sustain the increased loads. Considering all these, the taller tower and deeper foundation demand more materials as the initial investment (CAPEX) for larger diameter turbines is significantly higher as cost increases cubically with diameter. However, this initial cost could be offset by higher energy yield at lower wind speeds. At the same time, it is more viable financially to place this turbine in high wind speed sites where power generation is predictable.

1.4 BEMT vs CFD

Ashes implements Blade Element Momentum Theory (BEMT) to model the aerodynamic loads sustained by the rotor by dividing each blade into aerodynamic stations and computes the lift and drag forces based on local flow conditions. Another approach is to use Computational Fluid Dynamics (CFD) and both of these approaches differ in modelling fidelity and speed for aerodynamic analyses for an isolated wind turbine.

BEMT is used in ASHES to calculate the aerodynamic forces by assuming the flow over the rotor disk is uniform and axisymmetric as it segments blades into independent 2D elements. The flow on each blade element is independent of other sections and relies on 2D aerofoil data which leads to underpredicting the actual power output and the torque of the turbine. Moreover, it neglects 3D effects such as radial flow and tip vortices. This method also cannot model a turbulent region behind the rotor and dynamic stall condition thus cannot be used in wind farm modelling [6].

In contrast CFD offers higher fidelity by solving the full Navier Stokes equations, accurately capturing the 3D flow field, such as turbulence, boundary layer effects and wake structures around the turbine. It provides detailed information on pressure distribution, flow separation and unsteady effects making it suitable to analyse turbulent interactions between turbines in a wind farm. For an isolated wind turbine, CFD can resolve tip vortex structures as BEMT approximates it, these improved predictions of power output by 8% in ramp-up regions [7].

BEMT analysis is significantly faster because of the assumptions of the flow physics stated above. Simulating an isolated turbine can be completed in seconds to minutes on a standard computer. Due to this low computational cost this is ideal for the preliminary design stage as it requires many iterations and simulations. This speed essentially stems from avoiding detailed flow field calculations.

CFD on the other hand is computationally expensive and time consuming. Simulating a turbine can take hours or even days on a supercomputer as it greatly depends on the mesh resolution and the iterative manner of solving. Although CFD offers more detailed and accurate results, the computational demands make it impractical to do iterative design studies as well as the slow speed. However, this method is mainly used for validation and detailed design stages.

2. BLADE STRUCTURAL CHECKS

2.1 Blade–Tower Clearance

The minimum blade-tower clearance was determined under uniform flow at the rated windspeed of 12.5m/s, yielding a clearance of 9.37m. This was found by finding the Euclidean distance between the nodes and estimated the surface clearance shown in Figure 3. As per IEC 61400-1, the clearance must exceed 30% of the undeflected blade tip to tower distance [8][9]. The required minimum clearance based on the tower top diameter and rotor is 13.8m. The clearance found falls below this and consequently risking blade-tower strikes under extreme loads which causes structural failure.

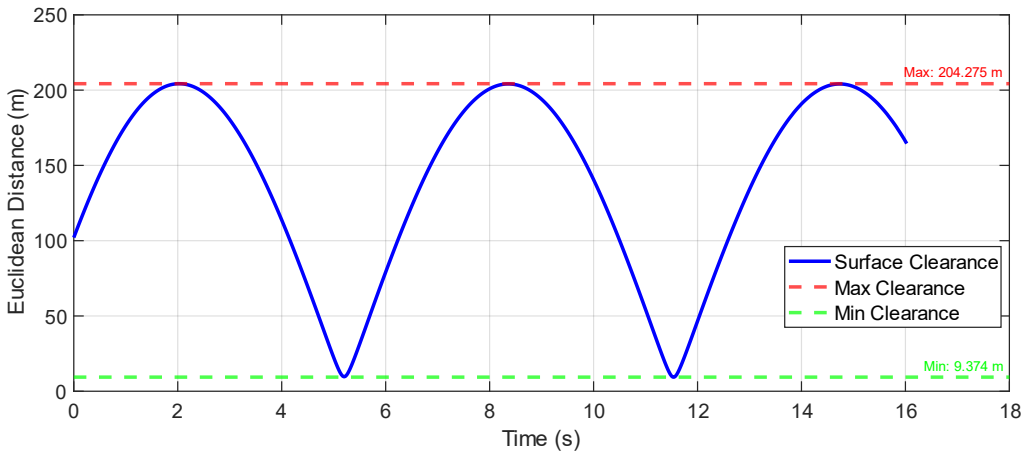

Figure 3: *The minimum surface clearance between the tower and the blade tip*

The three parameters that can be modified to adjust the clearance are blade stiffness, tower top diameter and rotor cone angle. Increasing the blade stiffness reduces the deflections under aerodynamic loads, which increases the clearance. However stiffer blades require aerofoil adjustments which potentially could reduce lift and reduce power output. The nacelle tilt angle moves the rotor plane upwind, increasing clearance but this reduces the effective rotor area perpendicular to the wind, lowering power output. Another parameter is the cone angle, increasing it moves the blade tip away from the tower, increasing clearance. Excessive coning, misaligns the blades with the oncoming wind flow increasing drag, reducing lift and the power coefficient. This reduces the AEP by 5% for a 2° increase beyond optimal [11]. Assumptions included uniform flow neglecting shear, a rigid tower and steady state operation at rated speed.

2.2 Evaluation of 2D Flapwise-Edgewise Blade Root Load Envelope

This load envelope was evaluated under extreme turbulent simulations as per DLC 1.3. It was defined in a polar coordinate system with 12 directions, plotting flapwise and edgewise moments. Simulations were done across 9 wind speeds from 5m/s to 25m/s with 600 turbulent wind files. A convergence analysis at 19.5m/s confirmed four simulations suffice as the max envelope moment stabilised at 69,126.34Nm and was within the tolerance of 5% as shown in Table 3. A 34x34 grid was chosen as the minimal uniform cell spacing of $1/30^{th}$ of the 208m rotor diameter according to the grid resolution study balancing accuracy and computational cost [12].

Figure 4 shows the polar load envelope which was built from the in-plane, out of plane bending moments, pitch and a constant twist angle of 14.5 at different windspeeds and was transformed to flapwise and edgewise moments. The overall envelope peaks at 95kNm dominated by 12.5m/s in the flapwise direction. The turbine operates at peak efficiency with maximum thrust and torque. Moreover, the pitch is 0° so this maximises flapwise bending but increases cyclic loading which leads to fatigue. The envelope peaks at 40kNm because of the 25m/s and remains dominant throughout 270°. The pitch adjustments cause a reduction in the lift to shed excess loads, and the inertial forces increases causing edgewise bending. At lower windspeeds, the moments are lower because of the reduced aerodynamic forces produced.

***Table 3**: Convergence Analysis at 19.5m/s*

Simulations	Max Moment (Nm)	% Change
1	60548.4	-
2	67633.5	11.70%
3	69362.5	2.56%
4	69126.3	0.34%

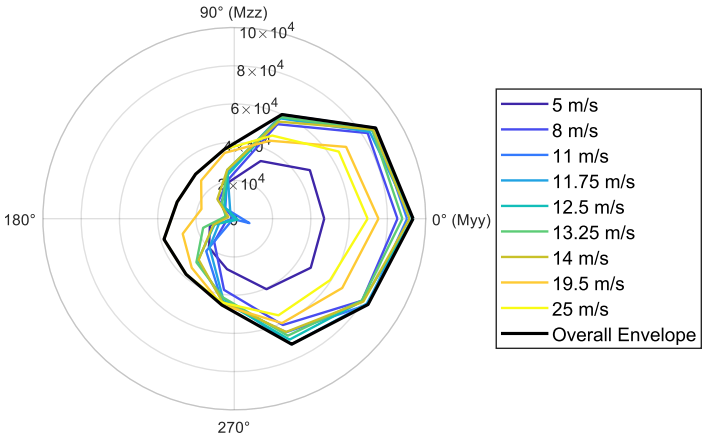

***Figure 4:** Polar Load Envelope from four Turbulent Simulations in Nm*

2.3 Wind Turbine Loads Under Uniform and Turbulent Flow Conditions

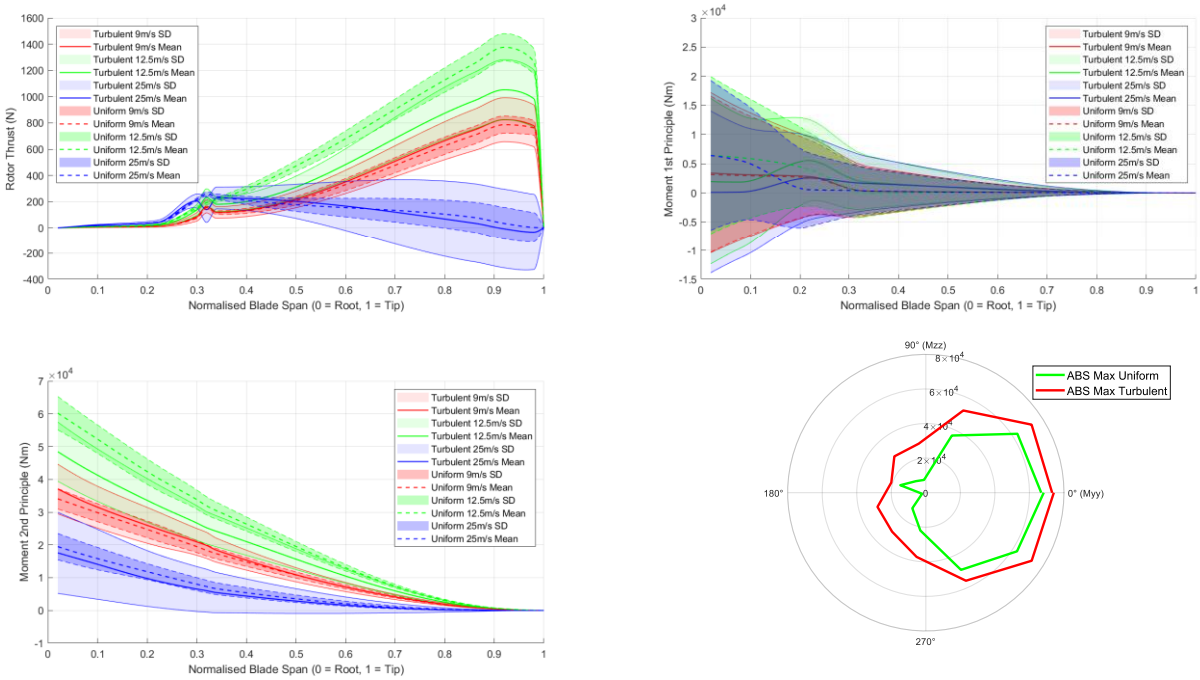

***Figure 5**: (a) Thrust (b) Flapwise (c) Edgewise bending moments comparison between uniform and turbulent conditions (d) Polar plot of Maximum of Turbulent and Uniform*

Thrust, flapwise and edgewise moments were compared between uniform and turbulent flow with three different windspeeds of 9m/s, 12.5m/s and 25m/s as shown in Figure 5. The mean thrust under turbulent flow at 12.5m/s is lower than the uniform flow due to the turbulent fluctuations. However, standard deviation is significant increasing fatigue risk with cyclic loading. The mean flapwise moment at the root under turbulent flow is similar to uniform flow as lift dominates both cases. The standard deviation of turbulent is higher as it is driven by gust induced angle of attack variations, elevating peak loads at the root of the blade. In the edgewise moment the mean at the rated speed is the highest and the lowest is the cut-out speed. This is because the blade pitches but still max moment occurs at the root. Standard deviation is very similar because the edgewise loads are less affected by aerodynamic fluctuations.
The polar plot at the bottom right corner shows that the turbulent conditions expand the load envelope with maximum moments by around 20% compared to the uniform. Turbulence

increases load variability, elevating fatigue and extreme loading cases. Uniform flow underestimates these effects making turbulent simulations critical for realistic structural design.

2.4 Axial Strain

The most critical structural areas were determined using the minimum and maximum axial strains caused by the combined flapwise and edgewise bending moments as failure indicators shown in Equation 2.1. Figure 6 shows that the maximum strain peaks at 0.65 span from the root. It decreases gradually as moments reduce due to the tapered blade. The minimum strain exhibits a kink at 0.1 span then continues decreasing as there is a structural transition between the root and the blade as there is a thinner cross section. The strain profile resembles the blade's physical shape with a sharp increase at 0.1 span and a peak at 0.7. at 0.1 span the maximum strain rises sharply from 0.00034 to 0.00061 which is due to the structural transition like a change in the cross-sectional geometry near the root hub connection. This analysis assumes a simplified cross sectional rectangular model with pseudo dimensions neglecting shear strains and torsional effects for simplicity. The uniform loading maximises aerodynamic loading providing a conservative estimate of strain. The blade's design was influenced the load distribution.

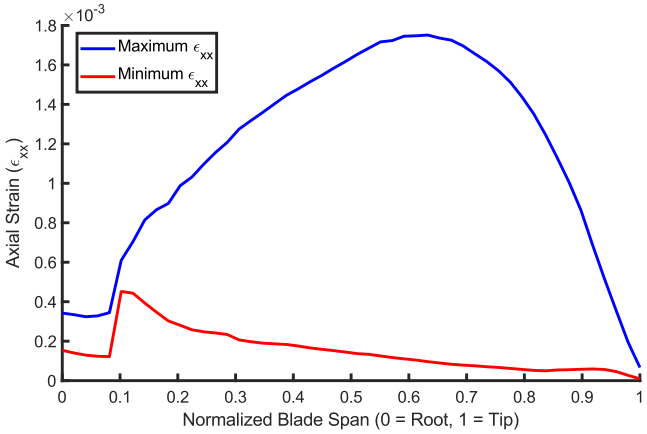

$$\epsilon_{xx} = -\frac{M_{zz}}{EI_{zz}} y_1 + \frac{M_{yy}}{EI_{yy}} z_1 \quad (2.1)$$

Figure 6: *Axial Strain Distribution Along Blade Span*

3. TOWER AND FOUNDATION DESIGN

3.1 Tower Design and Assumptions

This section presents the structural and dynamic checks of the wind turbine tower. It is a tapered steel structure designed to support the RNA model under the cut-out wind speed of 25m/s. Assumptions include fixed tower at the seabed in 40m water depth, uniform wind of 25m/s, a regular wave load with a mean height of 6m and a period of 10s, ignoring fatigue and secondary steel features, and a lumped mass RNA model thus considering a simple loading scenario. The tower dimensions chosen are listed in Table 4.

Table 4: *Tower Dimensions and Utilisation Factors*

Section	Height (m)	Diameter (m)	Thickness (m)	Utilisation Factors
Base	0	7.00	0.100	0.608
Mid-height	62.5	5.64	0.076	0.647
Top of Tower	125	3.08	0.031	0.357

3.1.1 Structural Checks

The tower, fixed at seabed, was analysed at three sections: the base, mid-height (82.5 m from the base or 42.5 m above the water level), and the top. The loads extracted included axial, shear forces, torque and bending moments. Additionally, cross-sectional properties of these elements such as area, moment of inertia, radius and thickness were obtained for each section reflecting the tapered tower geometry. These were then used to calculate the stresses using the equations

below. These stresses were used to determine the utilisation ratio at each section, ensuring the design withstands the applied loads. The partial safety factor was taken to be 1.15 as required by IEC-61400-1 [8].

$$\tau_{shear} = \left[\frac{V_b}{\pi r t}\right] sin\alpha \quad (3.1) \qquad \tau_{torsion} = M_T/2\pi t r^2 \quad (3.2)$$

$$\sigma = \frac{N_B}{A} + \frac{M_B}{I} r \quad (3.3) \qquad \sigma_{von-mises} = \sqrt{{\tau_{shear}}^2 + {\tau_{torsion}}^2} \quad (3.4)$$

Figure 7 plots the meridional, shear, torsional and Von-Mises stresses over a period of 120s. The utilisation factor was calculated at the three sections using peak stresses at 25 m/s. The maximum value was selected over the steady-state value to conservatively account for transient dynamic effects. This ensures the design withstands the highest loads encountered, aligning with standard practice for ultimate strength checks in wind turbine towers. The peaks are due to the pitch angle adjustment from the PID controller. The low utilisation factors indicate the tower has been overdesigned, reducing the diameter or thickness of the tower increases the utilisation factor and will lower CAPEX (Capital Expenditure) but risks buckling and fatigue as per Eurocode 3 [10]. At rated windspeed, the Von Mises stress peaks due to the 0° pitch angle, which maximizes aerodynamic forces on the blades, leading to higher stress levels. In contrast to cut-out speed because the pitch angle increases to reduce the aerodynamic loading on the blades. The fixed seabed assumption assumes infinite stiffness in the soil and overestimates structural resistance. Ashes lumped mass model simplifies stresses distribution which underestimates local peak stresses.

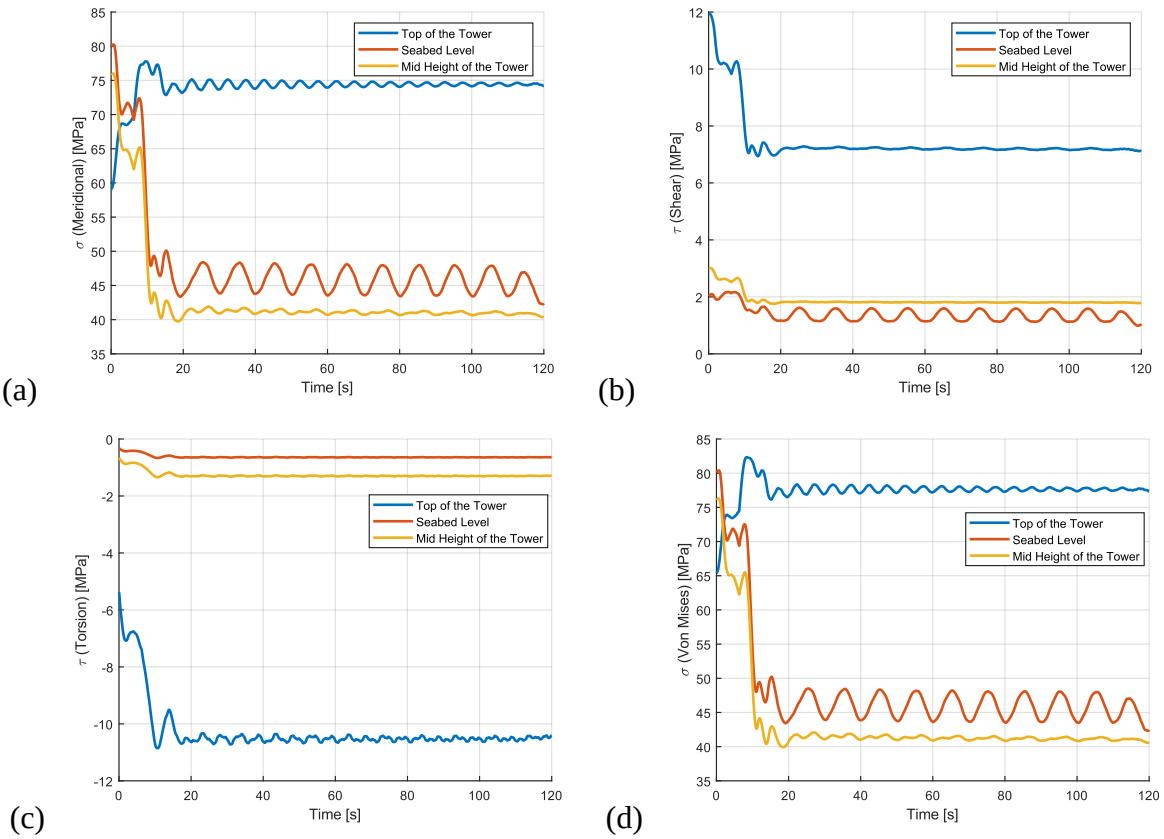

Figure 7: *Loading time histories at three tower sections. (a) Meridional, (b) Shear, (c) Torsional, (d) Von Mises stresses, with maximum used for utilisation ratios.*

3.1.2 Modal Analysis

The modal analysis was conducted in Ashes to generate the Campbell diagram and a normalized power spectral density graph which assesses resonance risks with rotational harmonics, wave and wind loadings. Both are shown in Figure 8.

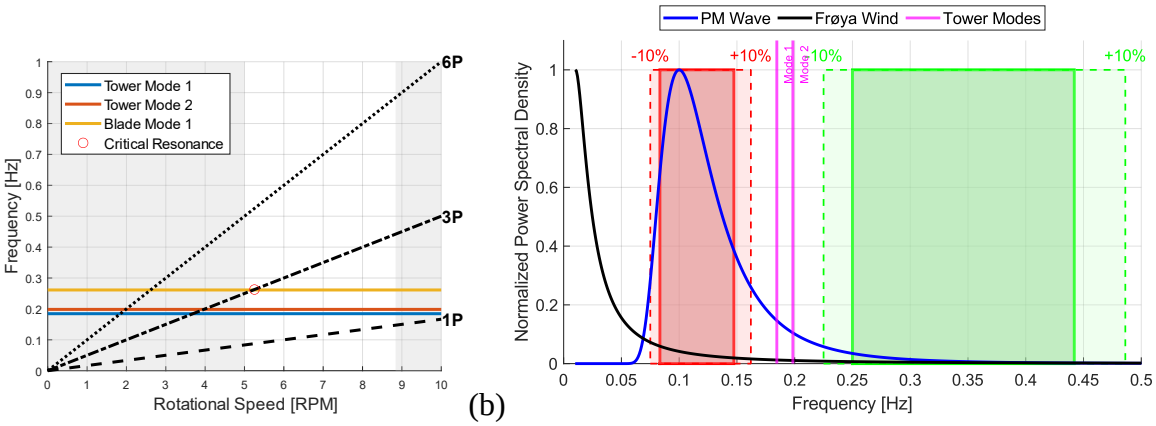

Figure 8: *(a) Campbell diagram: Tower and Blade frequencies vs RPM (b) Power Spectral Density vs Frequency*

3.1.3 Tower Design Region

The tower was evaluated to be in the soft-stiff design region based on the natural frequencies relative to the rotor's operational harmonics (1P and 3P). The modes and regions are listed in Table 5 below.

Table 5*: Natural Frequencies and Rotor Harmonics.*

Region	Modes	Natural Frequencies (Hz)
Tower	Side-Side	0.185
Tower	Fore-Aft	0.198
Blade	Edgewise	0.261
Harmonic	1P Range	0.075-0.162
Harmonic	3P Range	0.225-0.486

Being in this soft-stiff design region, it positions the natural frequencies outside the forbidden 1P region where continuous rotor excitation can amplify vibrations, yet below 3P avoiding higher harmonic conditions. It avoids direct resonance with the 1P harmonic which could amplify lateral tower deflection. Moreover, it also avoids the 3P band which will lead to stress concentrations and fatigue damage. A soft-soft design (below 1P) risks excessive flexibility and resonance with low-frequency wave loading, while a stiff-stiff design (above 3P) increases material costs without dynamic benefit. The soft-stiff approach balances structural efficiency and stability, as the tower avoids alignment with the dominant 1P harmonic while remaining clear of wave-induced excitation and also optimises material usage and costs. The forbidden regions are highlighted in Figure 8 in green and red. This placement of the tower modes minimises the risk of resonance induced vibrations due to environmental excitation from the wind and wave. Resonance occurs if the tower modes overlap the forbidden frequency bands as it amplifies vibrations and will lead to structural failure. Safety margins of 10% are plotted in the graph and the tower modes are still well away from it.

As shown in the Campbell chart in Figure 8, no tower frequencies coincide with 1P but does with the 3P but well below the operating RPM region. However, 3P coincides with the blade mode at RPM of 5.25 which will amplify blade and tower vibrations and leading to increase in fatigue loads due to higher stresses. Resonance magnifies the cyclic stresses which reduces the fatigue life of the blade, and this can lead to material cracking and delamination of composites. This resonance point, at RPM 5.25 represents a critical operating speed where the turbine

experiences higher fatigue loads, potentially shortening its service lifespan [13]. There is no frequency overlap for 6P.

3.1.4 Mitigation Measures for Resonance

The blade mode resonance at 5.25 RPM poses the greatest structural risk because it coincides with 3P harmonic. This leads to increases blade deflections, causing higher dynamic loads on the blade root. Although the tower modes do not coincide with 3P harmonic the blade resonance will transfer the loads to the tower and in turn increasing its bending moments. This reduces the fatigue life of the tower and the service lifetime.

Mitigations for the blade and tower vibrations include, increasing the stiffness of the tower by increasing the base diameter or increasing the blade stiffness. This will shift the blade mode frequency upward moving away from the 3P harmonic. However, this leads to increased material costs (increased CAPEX). Another mitigation is to introduce structural damping in the blade root or nacelle as the resonance point is on the natural frequency of the blade but it may contribute to the tower too so we also can add a damper at the tower. This will reduce the fatigue stress cycles extending the service life. The best mitigation for this design is to implement active RPM control as the resonant point is at 5.25 RPM so the controller can rapidly transition through this speed as the initial RPM is 5.

3.2.1 Monopile Design

The monopile geometry was defined using the tower base dimensions from Section 3.1 and summarised in Table 6 as well as the soil properties. The monopile was designed for a uniform clay seabed with an undrained shear strength (S_u) of 300kPa using a simplified API hard clay model to represent the soil reaction. A simplified geotechnical design analysis was conducted to determine the required monopile length needed to keep the pile head rotation below the tolerable limit of 0.5°. The analysis considered the maximum lateral load and bending moment at the seabed level under the cut-out wind speed of 25m/s. For a 40m monopile the rotation was 0.33°. The pile length was reduced until the 31m and was found to pass the limit which shows that the monopile has insufficient lateral resistance. Figure 9 below shows the pile deflection with the shear force applied for different monopile lengths. Assumptions include uniform soil, no partial safety factors, simplified API p-y curves and simplified loading scenario and no change in S_u with depth.

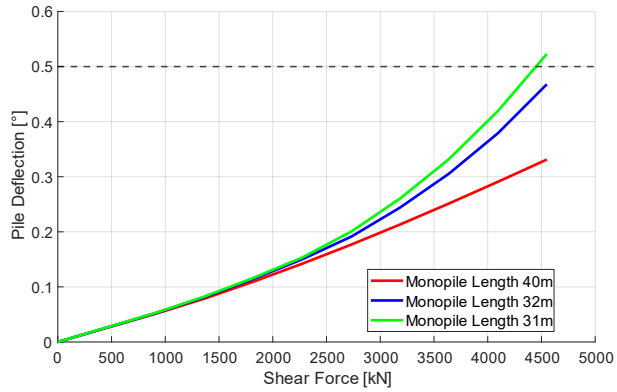

Figure 9: *Pile Deflection Analysis*

Table 6: *Monopile Dimensions and Soil Characteristics*

Parameter	Value
Length	40 m
Diameter	7 m
Thickness	0.1 m
Bending Stiffness (EI)	2709.678 GNm^2
Max Lateral Load at Seabed	4550 kN
Max Moment at Seabed	772000 kNm^2
Soil Type	Hard, stiff clay
Undrained Shear Strength (s_u)	300 kPa
ε_{50}	0.004
Clay unit weight (γ)	16 kN/m^3
Soil Resistance (p_u)	1.89×10^7 kN/m

3.2.2 Monopile Structural Check

Figure 10 below compares the current 40m monopile design, with a diameter of 7m, to the optimised design of 32m length maintaining the same diameter. The current design is represented with the red line while the optimised is shown on the blue line. Despite the optimisation, the 40m monopile will be used in the following sections.

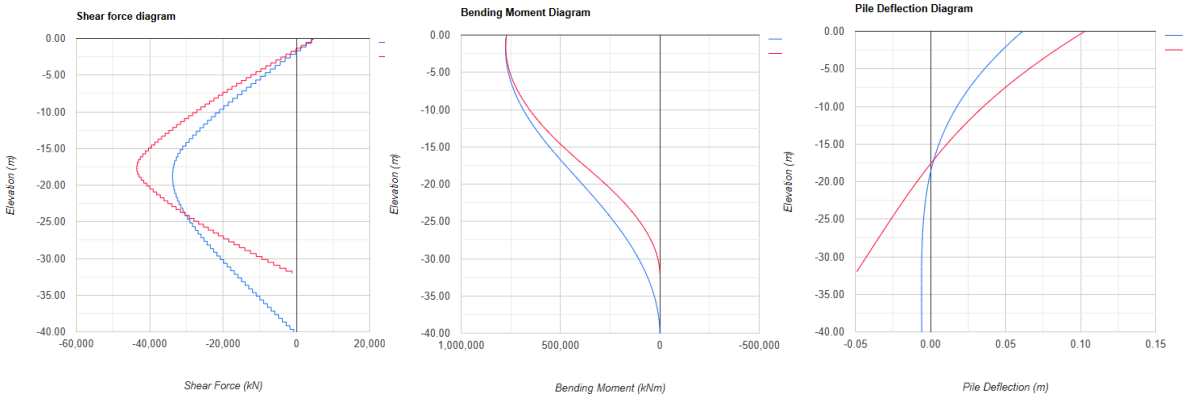

Figure 10: *Shear, Bending Moment and Pile Deflection Diagrams [14]*

The maximum lateral displacement occurs at the top of the monopile where the moment and lateral forces are the highest. The maximum shear force experienced by the monopile is at the halfway point of the length of the monopile. And the bottom of the monopile experiences the largest bending moment because that's where the lateral loads act.

Table 7: *Structural Check for Monopile*

Parameter	**Value**
Maximum Normal Stress	211MPa
Tau Shear	4.14MPa
Tau torsion	101MPa
Tau	101MPa
Von Mises	274MPa
Utilisation Factor	0.771

Table 8: *Natural Frequencies of different systems*

Configuration	**Mode 1 (Hz)**	**Mode 2 (Hz)**
Tower without monopile	0.185	0.198
Tower with monopile	0.149	0.152
Tower with monopile and soil stiffness	0.163	0.168

3.2.3 Natural Frequency of the Tower with the Monopile

The soil stiffness used in this analysis was 18900kN/m based on the deep failure formula in Equation 3.5. This was inputted into Ashes to conduct the eigenmode analysis. In the simulation, a vertical offset was applied to show the monopile's embedded length of 40m into the hard, clay soil. The tower modes were found to be close to the 1P region, still in the soft-stiff design region. Table 8 summarises the lowering of natural frequency when the monopile was added because of the added flexibility which lowers the overall stiffness in the tower-foundation system. Conversely, when the soil stiffness was added there was a slight increase in frequency because the soil provides additional resistance against lateral movement thus increasing the overall stiffness of the system. Figure 11 shows the design still remains in the soft-stiff design region but ever so close to the limits of 1P resonance region.

$$p_U = 9S_U D = 18900kN/m \qquad (3.5)$$

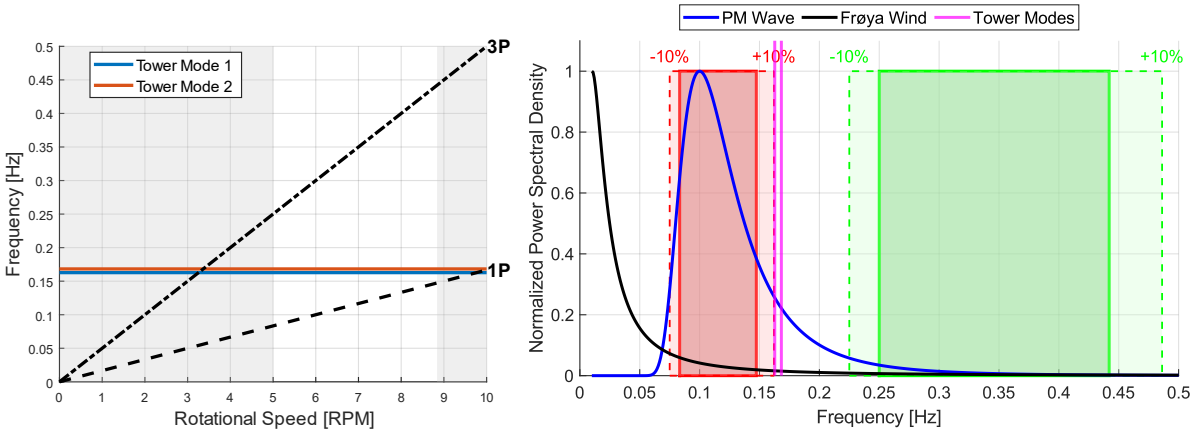

Figure 11: *Final Design Analysis of the Campbell and PSD*

3.2.4 Factors influencing Natural Frequencies and Soil Stiffness Effects

The natural frequencies of the tower are affected by loads such as wind, wave and rotor induced vibrations. Larger rotor diameters and longer blades increases the mass and the flexibility of the turbine thus lowering natural frequency. It is the same for using a heavier mass and more flexible blades, it lowers the frequency. In this simulation the mass of the nacelle is concentrated at the hub height which lowers the first natural frequency of the tower. However, larger turbines are more prone to resonance risks in the lower harmonic regions. A taller and more slender tower will have a lower stiffness resulting in lower natural frequencies thus being more susceptible to resonance in the 1P region. The Young's modulus of the material also affects the stiffness with stronger material results in higher natural frequency.

The foundation design and type also affect the overall stiffness such as jacket, monopiles, gravity based. Monopiles introduce flexibility at the base whereas jackets provide more rigidity and increase frequency. Stiffer soils increase frequency. A longer and wider monopile embedded provides more lateral resistance thus increasing the natural frequency

Soil Stiffness

The soil stiffness may change over the lifetime, because of the cyclic loadings from the wind and waves. It may compact the clay increasing its shear strength and stiffness over time. This will lead to an increase in the tower natural frequency. However, for specifically for offshore wind turbines, erosion of soil around the pile base due to currents reduce the effective embedment depth, lowering stiffness and frequencies [15]. Additionally, long-term soil fatigue or pore pressure changes in clay under repeated loading might soften the soil, further decreasing frequencies.

If over time the soil hardens it is best to design the tower with the natural frequency towards the left of the soft-stiff design region as it becomes stiffer the natural frequency would increase This design was built for soil hardening as the tower modes lay close to the 1P region.

REFERENCES

[1] Development of an Integrated Extreme Wind, Wave, Current, and Water Level Climatology to Support Standards-Based Design of Offshore Wind Projects Technology Assessment and Research Project #672 IEC 61400-3 Table 1 Design Load Cases (DLCs) APPENDIX A

[2] Research Hubs. (n.d.). *Power output variation with wind speed*. Available at:https://researchhubs.com/post/engineering/wind-energy/power-output-variation-with-windspeed.html#:~:text=The%20speed%20at%20which%20the%20turbine%20first%20starts,typically%20between%203%20and%204%20metres%20per%20second.

[3] Wind Turbine Models. (n.d.). *Mingyang MySE 16.0-242*. Available at: https://en.wind-turbine-models.com/turbines/2338-mingyang-myse16.0-242

[4] GE Vernova. (n.d.). *Haliade-X offshore turbine*. Available at: https://www.gevernova.com/wind-power/offshore-wind/haliade-x-offshore-turbine

[5] Siemens Gamesa. (n.d.). *SG 14-222 DD wind turbine*. Available at: https://www.siemensgamesa.com/global/en/home/products-and-services/offshore/wind-turbine-sg-14-222-dd.html

[6] Lin, L., 2016. BEMT and CFD-based unsteady aerodynamic analyses of floating offshore wind turbine.

[7] Menter, F.R., 2009. Review of the shear-stress transport turbulence model experience from an industrial perspective. *International journal of computational fluid dynamics*, *23*(4), pp.305-316.

[8] **International Electrotechnical Commission (IEC), 2019.** *IEC 61400-1:2019 – Wind energy generation systems – Part 1: Design requirements.* IEC Webstore. Available at: https://webstore.iec.ch/Home/IEC61400-1:2019

[9] **Germanischer Lloyd (GL), 2010.** *Guideline for the Certification of Wind Turbines.* Available at: https://wordpressstorageaccount.blob.core.windows.net/wp-media/wp-content/uploads/sites/649/2018/05/Session_3_-*Handout_3-*_GL_Guideline_for_the_Certification_of_Wind_Turbines.pdf

[10] **European Commission.** (n.d.) *Eurocode 3: Design of steel structures*. Available at: https://eurocodes.jrc.ec.europa.eu/EN-Eurocodes/eurocode-3-design-steel-structures

[11] Landahl, M.T., 1958. Calculation of stresses and natural frequencies for a rotating propeller blade vibrating flexurally. *Journal of Research of the National Bureau of Standards*, 21(5), pp.639-644. National Bureau of Standards.

[12] Van Der Laan, M.P., Storey, R.C., Sørensen, N.N., Norris, S.E. and Cater, J.E., 2014, June. A CFD code comparison of wind turbine wakes. In *Journal of Physics: Conference Series* (Vol. 524, No. 1, p. 012140). IOP Publishing.

[13] Qin, C.C., Loth, E., Zalkind, D.S., Pao, L.Y., Yao, S., Griffith, D.T., Selig, M.S. and Damiani, R., 2020. Downwind coning concept rotor for a 25 MW offshore wind turbine. *Renewable Energy*, *156*, pp.314-327.

[14] https://www.geocalcs.com/lap

[15] BSEE (Bureau of Safety and Environmental Enforcement), 2007. *Offshore Wind Turbine Development: Structural and Foundation Issues*. Technical Assessment Program, Report No. 672AA. Available at: https://www.bsee.gov/sites/bsee.gov/files/tap-technical-assessment-program/672aa.pdf